

This work is on a Creative Commons Attribution-NonCommercial-NoDerivatives 4.0 International (CC BY-NC-ND 4.0) license, <https://creativecommons.org/licenses/by-nc-nd/4.0/>. Access to this work was provided by the University of Maryland, Baltimore County (UMBC) ScholarWorks@UMBC digital repository on the Maryland Shared Open Access (MD-SOAR) platform.

Please provide feedback

Please support the ScholarWorks@UMBC repository by emailing scholarworks-group@umbc.edu and telling us what having access to this work means to you and why it's important to you. Thank you.

Online Supplement for

Real-time local oxygen measurements for high resolution cellular imaging

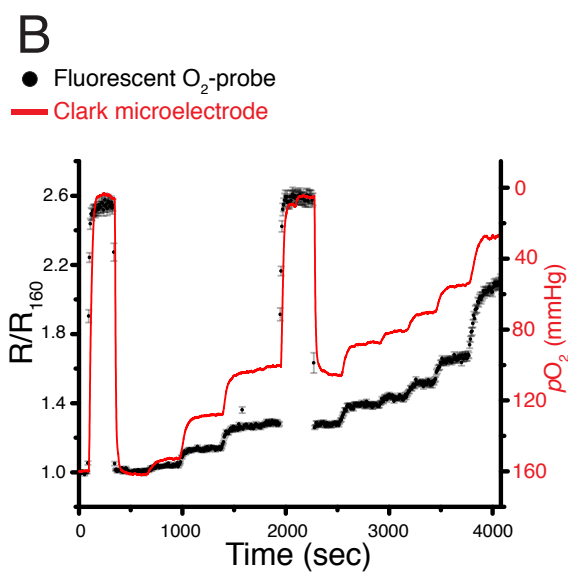
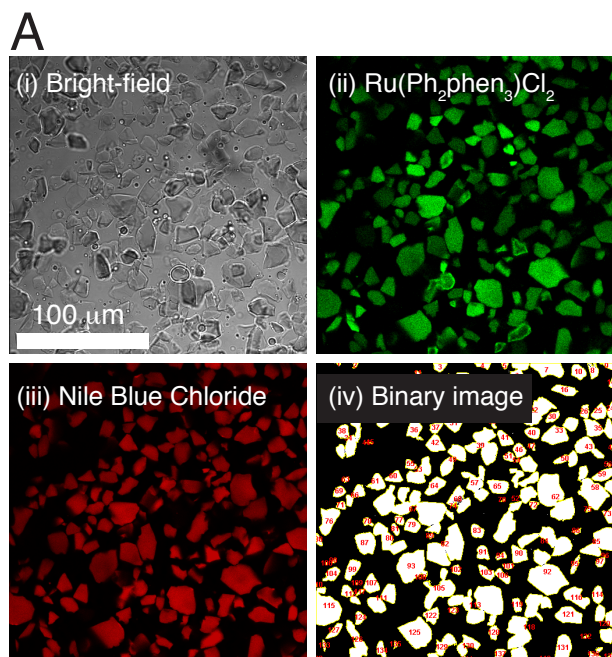
Liron Boyman, George S. B. Williams, Andrew P. Wescott, Jennie B. Leach, Joseph P. Y. Kao, W. Jonathan Lederer.

Supplementary Methods

Preparation of the encapsulated fluorescence oxygen-sensing microparticles. The oxygen-sensitive fluorophore tris-(BATHOPHENANTHROLINE) ruthenium (II) dichloride, or $\text{Ru}(\text{Ph}_2\text{phen}_3)\text{Cl}_2$ (GFS Chemicals, Powell, OH) and the oxygen-insensitive fluorophore Nile blue chloride (GFS Chemicals, Powell, OH) were immobilized to 9.5-11 micrometer Silica particles (Sigma) (For additional details see Acosta et al., 2012⁹). Fluorophore-bound silica particles (50-200 mg) were thoroughly mixed with 1 g of poly(dimethylsiloxane) (PDMS) pre-polymer, and 0.1 g of curing agent was added (Sylgard 184 elastomer kit; Dow Corning, Midland, MI). A single droplet (5 - 10 μL) of the resulting liquid slurry is gently compressed between two 21 mm microscope coverslips to obtain a thin planar PDMS coating. The two coverslips are separated and the PDMS coating is allowed to cure for 48 hours (hrs) at ambient room conditions. Note that, during the curing time each coverslip is oriented so that the PDMS coating is facing downward, this enables the Silica gel particles to settle close to the surface of the PDMS coating. After the 48 hr curing the coverslips are then baked at 60 °C for approximately 1 hr. After cooling at room temperature (~12 hrs) the coverslips are ready to be used.

Experimental apparatus. All solution perfusion lines are from O_2 -impermeable material (i.e., stainless steel tubing with polyether ether ketone (PEEK) fittings at the joints) and lead to a customized aluminium open-top chamber. The glass reservoirs containing the solutions are bubbled with gas mixtures, either high purity N_2 gas and air, or high purity Argon (Ar) and air. The gas purging ratio: N_2/air or Ar/air is set by two pressure regulators. When used, a commercially available, Clark-based dip-type, oxygen microelectrode (MI-730, Microelectrodes, INC, USA) is calibrated daily. The analog output (in mV) of the O_2 microelectrode is converted to $p\text{O}_2$ units (in mmHg) according to the manufacturer's instruction via two points calibration procedure, first by superfusing with air-saturated solution (160 mmHg), and then with Ar-saturated solution containing 20 mM sodium hydrosulfite ($\text{Na}_2\text{O}_4\text{S}_2$), which is taken as the anoxic point (~0 mmHg).

Confocal imaging. Imaging was done with a Zeiss LSM 510 inverted confocal microscope. $\text{Ru}(\text{Ph}_2\text{phen}_3)\text{Cl}_2$ is excited via the Argon 488 nm laser (505-530 nm emission) and Nile blue chloride via the HeNe 633 nm laser (505-530 nm emission). Ventricular myocytes were isolated using standard enzymatic approach¹⁰ from the hearts of adult (250-300 g) sprague dawley rats or new-zealand white rabbits. Cells were loaded with the acetoxymethyl ester form (AM) of the Ca^{2+} sensitive fluorescent indicator Rhod-2 (5 μM) for $[\text{Ca}^{2+}]_i$ transient measurements. Rhod-2 was excited via the HeNe 543 nm laser (560-590 nm emission). $[\text{Ca}^{2+}]_i$ transients were acquired using the linescan mode and analyzed using the image-processing software *ImageJ* ([Wayne Rasband, National Institutes of Health, Bethesda, MD](#)). Isolated cardiomyocytes are superfused with normal Tyrode (NT) as the extracellular (bath) solution, containing (in mM): NaCl (140), KCl (5), CaCl_2 (1.8), MgCl_2 (0.5), HEPES (5), Glucose (5), NaH_2PO_4 (0.33), pH 7.4 with NaOH. An ischemic Tyrode (IT) solution, is NT solution with the following modifications to simulate the ischemic conditions: 20 mM of NaCl are replaced with equimolar Na-Lactate, D-glucose is replaced by equimolar L-glucose, pH 6.8. All experiments were conducted at room temperature.

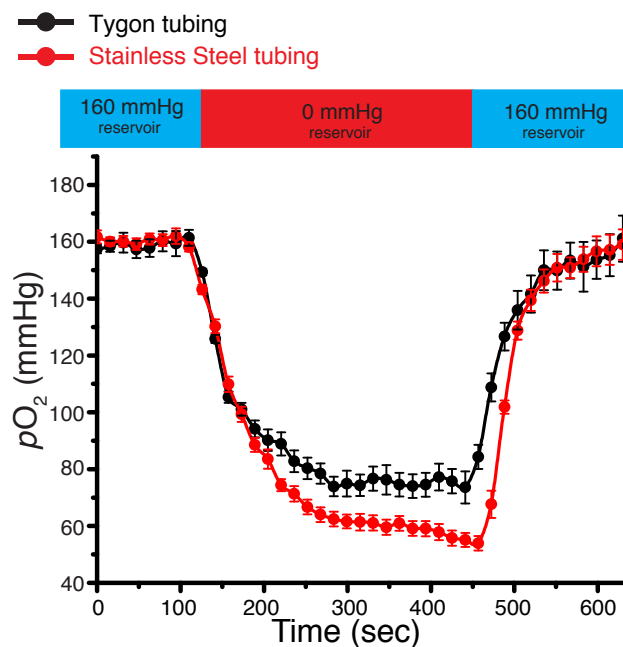


R/R_{160}	$p\text{O}_2$ (mmHg)	R/R_{160}	$p\text{O}_2$ (mmHg)
1.00	160	1.55	70
1.04	150	1.60	65
1.08	140	1.65	60
1.13	130	1.71	55
1.18	120	1.77	50
1.24	110	1.84	45
1.30	100	1.91	40
1.37	90	1.99	35
1.46	80	2.29	20
1.50	75	2.85	0

Supplemental Figure 1. Calibration of the O_2 -probe. (A) (i) Bright-field image showing the PDMS-encapsulated silica microparticles. (ii) Confocal image showing the fluorescence of the microparticles-bound oxygen-sensitive fluorophore $\text{Ru}(\text{Ph}_2\text{phen}_3)\text{Cl}_2$. (iii) Confocal image showing the fluorescence of the microparticles-bound oxygen-insensitive fluorophore Nile blue chloride. (iv) Binary image obtained by thresholding the fluorescence image of Nile blue chloride. Identified individual silica particles are superimposed with yellow borders. (B) Time-dependent fluorescence measurements of $p\text{O}_2$ with the silica oxygen-sensor (filled black circles, $n=107$ silica particles), and simultaneous measurements with a Clark oxygen microelectrode (red line) from a rapid superfusion chamber. The inset is showing the time-dependent fluorescence signals from $\text{Ru}(\text{Ph}_2\text{phen}_3)\text{Cl}_2$ (filled green circles, $n=107$ silica particles) and Nile blue chloride (filled blue circles, $n=107$ silica particles).

Supplemental Table 1. Conversion of the fluorescence signals from the O_2 -probe to $p\text{O}_2$.

Quantitative $p\text{O}_2$ values in mmHg obtained from the measured O_2 -probe signals (i.e., R/R_{160}). The conversion is done using previously attained calibration constants (i.e., $f_1=0.96$, $R_0/R_{160}=2.85$, $K_{\text{sv}}=0.013 \text{ mmHg}^{-1}$).

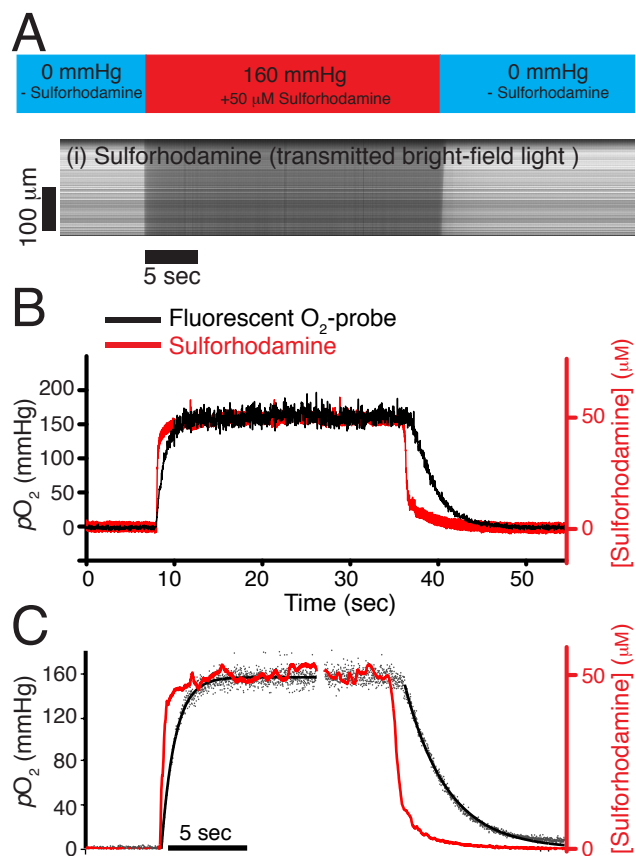


Supplemental Figure 2. Degradation of oxygen gradients by atmospheric O_2 .

Time-dependent measurements of local pO_2 with the O_2 -probe. Solutions are delivered from the reservoirs at the times indicated through either Tygon tubing (black circles) or stainless steel tubing (red circles).

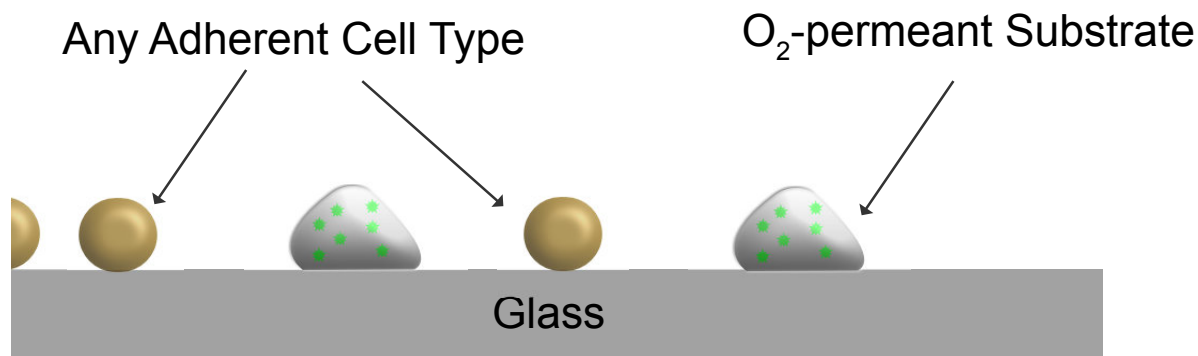
Material	Diffusion Coefficient (cm ² /s)	Temperature (C)	Reference
Stainless Steel	10^{-16}	23	[1]
Glass (SiO ₂)	10^{-15}	23	[2]
Poly(Ethel ether ketone) or PEEK	10^{-9}	25	[3]
Polycarbonate	3.53×10^{-8}	25	[3]
Tygon	10^{-7} - 10^{-8}	23	[4]
Polyethylene	10^{-7}	25	[5]
Polystyrene	1.1×10^{-7}	25	[6]
H ₂ O	2.4×10^{-5}	25	[7]
Polydimethylsiloxane or PDMS	3.55×10^{-5}	25	[8]

Supplemental Table 2. Oxygen diffusion rates through commonly used materials for cellular imaging systems. Diffusion constants for each material are taken from the references indicated and can be found in the SI.

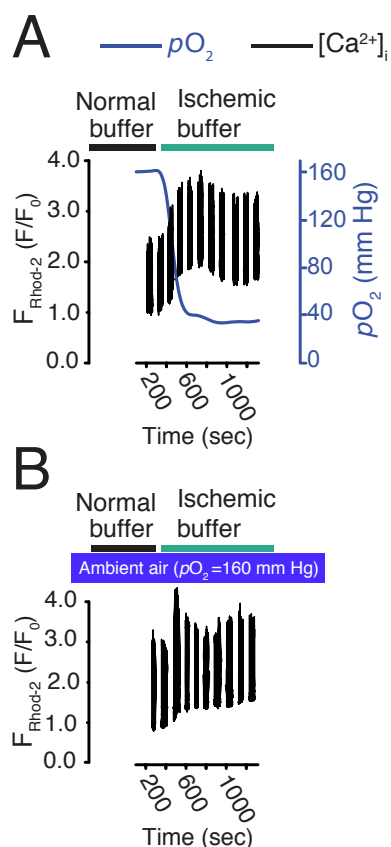


Supplemental Figure 3. Measuring the abrupt local (bathing) solution switch.

(i) bright-field line-scan image showing the abrupt local (bathing) solution switch from anoxic solution to hyperoxic (160 mmHg), and back again to anoxic solution. Note that the hyperoxic solution contained 50 μ M Sulforhodamine that reduces the transmitted light and is used here to measure the local switch between the two solutions. (B) The red line shows the time-course of changes in the local (bathing) solution. The black line shows the simultaneous pO_2 measurements with the O_2 -probe (8 O_2 -microsensors, from Fig 4A). (C) Black lines are double exponential fits to the pO_2 rise ($t_{0.5}=0.7$ sec, $n=6$ experiments) and pO_2 decay ($t_{0.5}=1.63$ sec, $n=6$ experiments). The red line shows the time-course of changes in the local (bathing) solution in these experiments.



Supplemental Figure 4. Diagram of method adapted for any cell type and use with or without confocal imaging capabilities.



Supplemental Figure 5. Cytosolic Ca^{2+} signaling in ventricular myocytes is sensitive to multiple ischemic factors. (A) The time course of changes of pO_2 (blue line) and cytosolic Ca^{2+} (black line). The Ca^{2+} -sensitive fluorophore Rhod-2 is used for cytosolic Ca^{2+} ($[Ca^{2+}]_i$) measurements. Fluorescence line-scan measurements of $[Ca^{2+}]_i$ are acquired along the longitudinal axis of a cardiomyocyte. During each imaging break as noted by the gaps in the records, the automated focal plane adjustment function of the confocal microscope switches back and forth between two planes. The two planes are: 1) the imaging plane of the cardiomyocyte and 2) the imaging plane of the OxySplots for pO_2 measurements. The cell is initially perfused with normal Tyrodes solution (i.e., Normal Buffer), and then perfused with ischemic buffer. Ischemic buffer is composed of normal Tyrodes solution in which 20 mM NaCl is replaced with equimolar Na-Lactate and D-glucose is replaced by equimolar L-glucose and acidity is adjusted to pH 6.8. The solution reservoir that holds the ischemic buffer is vigorously bubbled with pure Argon (99.99%) to reduce its pO_2 to near 0 mm Hg. During the entire time course of the experiment electric field shocks (stimulations) were applied at 0.5 Hz. Panel A was adapted from Figure 6 A and shown for comparison. (B) The experiment of panel (A) is repeated except that the pO_2 was maintained at 160 mmHg (room air) throughout the experiment.

Supplemental Movie 1. Time-laps confocal microscopy imaging showing the fluorescence of Nile Blue during abrupt changes of pO_2 from 160 to 0, and back to 160 mmHg.

Supplemental Movie 2. Time-laps confocal microscopy imaging showing the fluorescence of $Ru(Ph_2phen_3)Cl_2$ during abrupt changes of pO_2 from 160 to 0, and back to 160 mmHg.

Bibliography

1. A. Fattah-alhosseini MHA, and S. Banaei. Diffusivity of Point Defects in the Passive Film on Stainless Steel. *International Journal of Electrochemistry*. 2011;2011:6.
2. García-Rodríguez FJ P-RF, Manzano-Ramírez A, Vorobiev YV and González-Hernández. Oxygen diffusion in silica glass prepared by the sol-gel method. *Solid state communications*. 1999;111:717-721.
3. Monson L, Moon SI and Extrand CW. Permeation resistance of poly(ether ether ketone) to hydrogen, nitrogen, and oxygen gases. *Journal of Applied Polymer Science*. 2013;127:1637-1642.
4. Wilson RD and Mackay DM. Diffusive oxygen emitters for enhancement of aerobic in situ treatment. *Groundwater Monitoring & Remediation*. 2002;22:88-98.
5. Moisan JY. Effects of Oxygen Permeation and Stabiliser Migration on Polymer Degradation. In: J. Comyn, ed. *Polymer Permeability*: Springer Netherlands; 1985: 119-176.
6. Shlyapnikov YA, Kiryushkin SG and Mar'in AP. *Antioxidative stabilization of polymers*: CRC Press; 1996.
7. J GC. Transport Processes and Unit Operations. Prentice Hall International Series in the Physical and Chemical Engineering Sciences; 1993(Third edition).

8. Cox ME and Dunn B. Oxygen diffusion in poly (dimethyl siloxane) using fluorescence quenching. I. Measurement technique and analysis. *Journal of Polymer Science Part A: Polymer Chemistry*. 1986;24:621-636.
9. Acosta MA, Velasquez M, Williams K, Ross JM and Leach JB. Fluorescent silica particles for monitoring oxygen levels in three-dimensional heterogeneous cellular structures. *Biotechnol Bioeng*. 2012;109:2663-70.
10. Boyman L, Hiller R, Lederer WJ and Khananshvil D. Direct Loading of the purified endogenous inhibitor into the cytoplasm of patched cardiomyocytes blocks the ion currents and calcium transport through the NCX1 protein. *Biochemistry*. 2008;47:6602-11.